Jurnal Teknologi

Full Paper

MODIFIED ABSORPTION FEATURES OF TITANIA-ERBIUM INCORPORATED PLASMONIC TELLURITE GLASS SYSTEM

Nur Nabihah Yusof, Sib Krishna Ghoshal*, Ramli Ariffin, Mohd Rahim Sahar

Department of Physics, Advanced Optical Materials Research Group, Faculty of Science, Universiti Teknologi Malaysia, 81310 UTM Johor Bahru, Johor, Malaysia

Article history
Received
10 February 2015
Received in revised form
30 Mei 2015
Accepted
30 June 2015

*Corresponding author
sibkrishna@utm.my

Graphical abstract

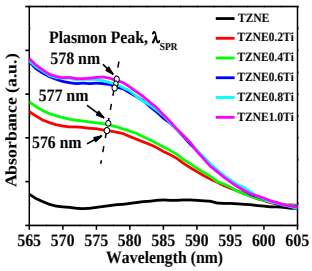

Abstract

Achieving efficient lasing glass materials with enhanced absorption and emission cross-section by reducing the Rare Earth (RE) concentration quenching is a challenging issue. Metal nanoparticles (NPs) together with RE ions in the glass matrix are thought as a suitable alternative to overcome the limitations of concentration quenching and weak absorption of inorganic glasses. We prepare a series of Titania-Erbium doped Tellurite glass system with the form $(69\text{-}x)TeO_2\text{-}20ZnO\text{-}10Na_2O\text{-}1Er_2O_3\text{-}(x)TiO_2$, where $0 \leq x \leq 1.0$ mol% via melt-quenching method with optimum erbium contents and varying TiO_2 NPs concentrations. The NPs concentration dependent modifications in the absorption characteristics are scrutinized. Glasses are characterized via UV-Vis-NIR and XRD measurements. XRD pattern verifies the amorphous nature of prepared samples. The incorporation of TiO_2 NPs is demonstrated to enhance the absorption intensity significantly. This augmentation is attributed to the effect of Surface Plasmon Resonance (SPR) mediated strong local electric field that is swallowed by neighboring Er^{3+} ions. The observed modification in optical energy band gap and Urbach energy are ascribed to the strong electric field around NPs that interact with the ligand of glass network to transform weak bond into defects. This observation is useful for the development of plasmonic nanoglass materials applicable for photonic devices.

Keywords: Tellurite glass, titanium dioxide nanoparticle, absorption spectra

Abstrak

Untuk mencapai bahan kaca pelaseran yang efisien dengan penambaikan daya penyerapan dan pancaran serta mengurangkan masalah penurunan keamatan pancaran Rare earth (RE) dalam kaca merupakan isu yang mencabar untuk ditangani. Logam Nanopartikel (NPs) bersama-sama dengan ion RE dalam matrik kaca dianggap alternatif yang sesuai untuk megatasi masalah penyerapan RE yang rendah dan penurunan pendarkilau RE dalam kaca. Satu siri kaca Titania-Erbium yang didopkan dalam kaca Tellurite telah dihasilkan dengan komposisi $(69\text{-}x)Te_2O\text{-}20ZnO\text{-}10Na_2O\text{-}1Er_2O_3\text{-}(x)TiO_2$, dalam julat $0 \leq x \leq 1.0$ mol% melalui kaedah pelindapkejutan-leburan dengan kandungan erbium yang optimum dan komposisi TiO_2 NPs yang pelbagai. Kadar penyerapan bahan kaca mengandungi komposisi TiO_2 NPs yang berbeza-beza diteliti. Kaca ini telah dicirikan menggunakan UV-Vis-NIR spektroskopi dan XRD. XRD telah mengesahkan sampel adalah bahan amorphous. Penambahan komposisi TiO_2 NPs didapati mampu meningkatkan kadar penyerapan kaca. Peningkatan penyerapan ini adalah disebabkan Resonan Permukaan Plasmon (SPR) yang menghasilkan medan elektrik setempat dan memindahkan tenaga kepada RE. Jurang jalur tenaga optik dan tenaga Urbach diamati. Parameter ini dipengaruhi oleh medan elektrik di sekitar NPs dalam rangkaian kaca dimana ikatan yang lemah akan diubah menjadi kecacatan. Kajian ini dipercayai bermafaat bagi memperluaskan pergunaan bahan kaca plasmonik dan bahan peranti fotonik

Kata kunci: Kaca tellurite, titanium dioxide nanopartikel, spectra penyerapan

© 2015 Penerbit UTM Press. All rights reserved

1.0 INTRODUCTION

Nowadays, the demand of rare earth (RE) doped glasses is exponentially growing especially for photonic applications including cheap solid state laser, optical amplifiers, non-linear optical devices, and production of optical fibers. Selecting host glasses for RE ions are important for efficient up-conversion emission [1]. Tellurite based-glass is the most promising host glass due to several special feature such as wide transmission range from UV to IR region (340nm-15μm), low dispersion, superior transparency with refractive index between 2 to 2.5, high earth ion solubility [2], good thermal stability, chemical durability and low melting point [3].

Meanwhile, erbium remains the most attractive luminescent rare-earth element due to its emission in visible region which is beneficial for laser development [4]. However, Er^{3+} has been disqualified to be nominated as strong emitter because of its small absorption and emission cross-section [5]. Several methods are proposed to overcome this drawback. The addition of second dopant either a REs or a transition metal which can enhance the optical properties of RE-doped glasses is suggested. Incorporation of metallic NPs into the glass are striking due to surface plasmon resonance (SPR) mediated impact on RE ions [6]. Apart from NPs manipulation and formation, glasses are the suitable dielectric host for activating enough RE ions via metallic NPs that act as sensitizers.

Silver and gold NPs is usually used as second dopant in Erbium-doped tellurite glass due to its chemical stability and strong SPR effect. However due to the wide range of parameters for separate applications, it is impossible to address all the requirements by use of silver and gold; therefore, alternative materials are needed to optimize the performance. Titanium NPs is attractive yet less exploited as second dopant in Erbium-doped tellurite glass even it exhibit SPR effect [7]. Metal oxide, TiO_2 NPs in the erbium-tellurite glass host is thought to offer high linear optical response [8] since the empty d-shell of Ti ion contribute strong linear polarizability [9]. Its oxide layer has advantage such as the position of SPR can be tuned by varying the thickness of oxide layer.

In addition, certain value of thickness of oxide layer can increase the SPR intensity instead of decreasing it. This effect make TiO_2 NPs more attractive for plasmonic and photonic application like solid-state laser [10]. Despite few systematic studies on titania-erbium doped tellurite glass, the mechanism of TiO_2 NPs stimulated spectroscopic modification is far from being understood.

We report the improvements in the absorption properties of TiO_2 NPs embedded erbium-doped tellurite glasses. TiO_2 NPs concentration dependent density, molar volume, optical energy band gap, Urbach energy, refractive index, and polarizability are determined. The synthesized disordered plasmonic media is demonstrated to be ideal for sundry nanophotonic applications.

Table 1 Compositions (in mol%) of synthesized glass samples and their codes

Glass	TeO_2	ZnO	Na_2O	Er_2O_3	TiO_2
TZNE	69	20	10	1	0
TZNE0.2Ti	68.8	20	10	1	0.2
TZNE0.4Ti	68.6	20	10	1	0.4
TZNE0.6Ti	68.4	20	10	1	0.6
TZNE0.8Ti	68.2	20	10	1	0.8
TZNE1.0Ti	68	20	10	1	1.0

2.0 EXPERIMENTAL

Series of glasses (enlisted in Table 1) with composition (69-x)TeO_2-20ZnO-10Na_2O-1Er_2O_3-(x)TiO_2 (where x ranges within 0 to 1.0 mol%) are synthesized using melt-quenching technique. Low doping level of Er^{3+} is maintained to avoid undesirable attenuations such as dipolar interaction and luminescence quenching. Analytical grade starting materials of TeO_2 (purity 99.5%), ZnO (purity 99.9%), Na_2O (purity 80.0%), Er_2O_3 (purity 99.9%) and TiO_2 (purity 99.7%) from Sigma Adrich are acquired as glass constituents and thoroughly grinded. A platinum crucible holding this constituents mixture are placed inside an electrical furnace at 900°C for 20 minutes to achieve complete molten state. The melt is poured in a brass mould before transferring to an annealing furnace at 300 °C for 3 hours to remove residual thermal and mechanical strains. The sample is then cooled down to room temperature and stored in a desiccator to prevent a moisture attack. Finally, they are cut and polished to a thickness 2.5±0.5 mm to produce shiny and scratch free surface for optical measurements.

The X-ray diffraction (XRD) measurements are performed using PANalytical X'Pert PRO MRD PW3040 with Cu Ka radiations (λ = 1.54 Å) in scanning angle of 2θ ranging between 10° and 80° operated at 40kV and 35 mA. Room temperature optical absorption spectra

are recorded in the wavelength range of 200-1800 nm using a Shimadzu UVPC-3101 spectrophotometer with resolution of ± 1 nm. The glass density is measured by Achimedes method via Analytical balance of specific density-Precisa XT 220A with distilled water as an immersion liquid. The density ρ (g/cm^3) of each sample is determined using the expression [11],

$$\rho = \rho_w \frac{W_a}{W_a - W_w} \quad (1)$$

where ρ_w is the density of distilled water (0.9975 g/cm^3) W_a and W_w are the weight of the sample in the air and in water respectively.

The molar volume V_m is calculated using [12] ,

$$V_m = \sum_i \frac{x_i M_i}{\rho} \quad (2)$$

where x_i and M_i denote the molar fraction and molecular weight of the ith component, respectively. The refractive index n of glasses are calculated following [13],

$$\frac{n^2-1}{n^2+2} = 1 - \sqrt{\frac{E_{opt}}{20}} \quad (3)$$

where E_{opt} is the optical band gap energy of the glass obtained from the absorption data. The molar refractivity R_m is obtained using [14],

$$R_m = \frac{n^2-1}{n^2+2}(V_m) \quad (4)$$

The polarizability α_e of the glasses is related to the refractive index through Lorentz-Lorenz equation and can be determined from [15],

$$R_m = \frac{4}{3} N_a \alpha_e \quad (5)$$

where N_a is the Avogadro's number.

The optical absorption coefficient $\alpha(\lambda)$ is calculated from the following expression [16] ,

$$\alpha(\lambda) = \frac{2.303A}{d} \quad (6)$$

where A is absorbance and d is the thickness of the samples. The optical energy band gaps for direct and indirect transitions and the Urbach energy are calculated using the UV absorption edge. The frequency dependent absorption coefficient $\alpha(\omega)$ yields [17],

$$\alpha(\omega) = \frac{B(\hbar\omega - E_{opt})^n}{\hbar\omega} \quad (7)$$

where B is a constant, E_{opt} is the optical band gap, $\alpha(\omega)$ is the absorption coefficient at an angular frequency $\omega = 2\pi\nu$, $\hbar$ is the Planck constant divided by 2π and n is the index can assume values of 0.5, 1.5, 2 and 3 depending on the nature of electronic transitions responsible for the absorption.

Urbach energy that characterizes the extent of the exponential tail of the absorption edge is given by [18]

$$\alpha(\omega) = B\exp\left(\frac{\hbar\omega}{\Delta E}\right) \quad (8)$$

where ΔE is Urbach energy.

3.0 RESULTS AND DISCUSSION

Figure 1 displays the typical XRD spectra of two Er^{3+} doped zinc-sodium tellurite glass samples containing titanium dioxide NPs. The presence of broad hump between 25° and 35° without any sharp crystallization peaks confirms the amorphous nature of these samples.

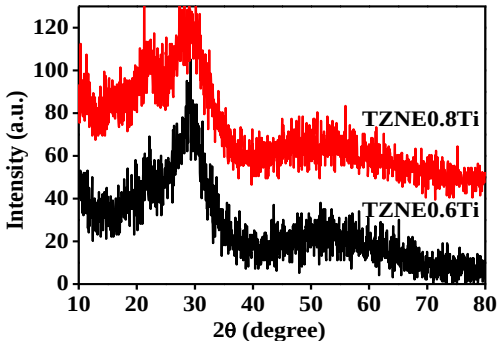

Figure 1 Typical X-ray diffraction pattern for two samples with different TiO_2 NPs content

Figure 2 illustrates the TiO_2 NPs concentration dependent variation of density and molar volume.The density is found to decrease with the increase of TiO_2 NPs contents up to 0.4 mol% and then increased thereafter. This reduction in density is attributed to the substitution of higher molecular weight TeO_2 (159.60 g mol^{-1}) compound by a lower molecular weight TiO_2 (79.876 g mol^{-1}) entity in the glass network. The weak connectivity in the glass structure causes a drop in the density [19]. Furthermore, the increase in density is due to the increase of the glass network rigidity and compactness of the glass [15]. The increase in molar volume reflects the enhancement of free volume.

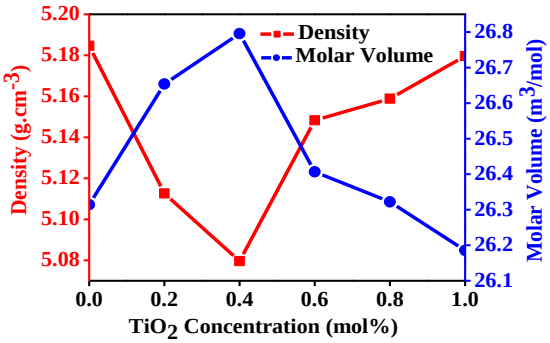

Figure 2 TiO_2 NPs concentration dependent changes in density and molar volume

Figure 3 shows the UV-Vis-NIR absorption spectra of all samples. Seven absorption bands centered at 448, 489, 524, 655, 803, 978 and 1530 nm corresponding to the transition from the $^4I_{15/2}$ ground state to $^4F_{3/2}$, $^4F_{7/2}$, $^4H_{11/2}$, $^4F_{9/2}$, $^4I_{9//2}$, $^4I_{11/2}$ and $^4I_{13/2}$ excited state respectively are evidenced. The weak absorption band at 550 nm is assigned to $^4S_{3/2}$ transitions which overlap with upper neighboring level of $^4H_{11/2}$ [20]. Spectral features of all samples are qualitatively similar except the variation in intensity. Addition of TiO_2 NPs caused red shift at the absorption edge [24] which attributed to the formation of non-bridged oxygen (NBOs) [2]. In fact, a structural rearrangement of the glass network occurred with the increase of TiO_2 NPs concentration [25]. Even though the Er^{3+} ions absorption bands overlapped the TiO_2 NPs resonance wavelength [26], however a weak plasmon band is detected in the range between 576-578 nm as shown in Figure 4. This weak band originated from TiO_2 NPs stimulated SPR effect [27].Resonances of coherent oscillation of the surface conduction electron of TiO_2 NPs with the incident electromagnetic radiation manifested this plasmon absorption band [28]. Moreover, the SPR band can be tuned by varying the shape and size of NPs [29] which in usually done by accurately changing TiO_2 NPs concentration, annealing temperature and time.

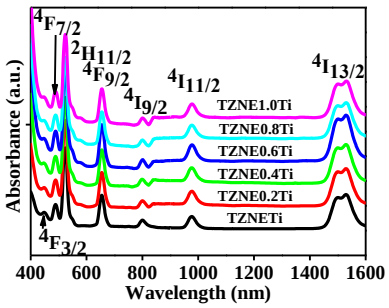

Figure 3 UV-Vis-NIR absorption spectra of glass samples in the range of 400-1600 nm

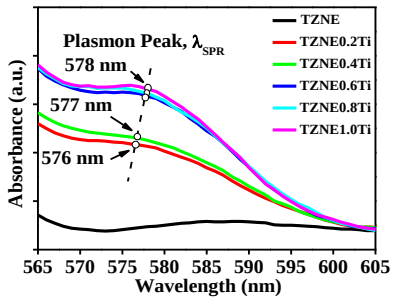

Figure 4 SPR band position of TiO_2 NPs

Optical transition and electronic band structure is analyzed using absorption spectra. Davis and Mott theory [17] is used to evaluate the optical band gap energy of the glass for both direct and indirect allowed transitions. In both transitions, the electromagnetic waves interact with the electrons in the valence band which are raised across the fundamental gap to reach the conduction band. However in amorphous material such as glass, indirect transition is most likely to occur and thus create band tail at the absorption edge. The Tauc's plot is drawn between $(\alpha\hbar\omega)^n$ and photon energy $(\hbar\omega)$ by substituting n = 2 for direct allowed transition and n = 1/2 for indirect allowed transitions. The optical band gap values is obtained from the tangential intercept extrapolated at $(\alpha\hbar\omega)^2$ = 0 and $(\alpha\hbar\omega)^{\frac{1}{2}}$ = 0 for direct and indirect transitions, respectively.

Figure 5 displays the TiO_2 NPs concentration dependent changes in the direct (3.17 - 2.98eV) and indirect (3.36 - 2.84 eV). Reduction in optical band gap energy is due to the decrease in the average of bond energy and glass compactness. The addition of TiO_2 NPs in the host glass causes the formation of the NBO and reduces the BOs abundance. The decrease of optical band gap is due to low bonding energies of NBOs [30].

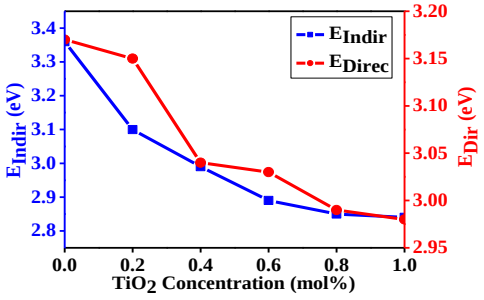

Figure 5 Indirect and direct optical energy band gap with different TiO_2 NPs concentration

Figure 6 represents the Urbach energy as a function of NPs contents. The value of $\alpha(\omega)$ near the absorption band edge exhibits an exponential behavior on the photon energy ($\hbar\omega$) and obeys the empirical relation given by Urbach [16]. The exponential behavior of the band tail is due to the extensions of the valence and conduction bands to the band gap region. Figure 4(b) clearly shows increase in the band tail from 0.13 to 0.33 eV with the insertion of TiO_2 NPs into the glass. Urbach energy is used as yardstick to measure disordered nature of glass. Glass with large Urbach energy have greater tendency to convert weak bonds into defects due increase of disorder in the glass [31].

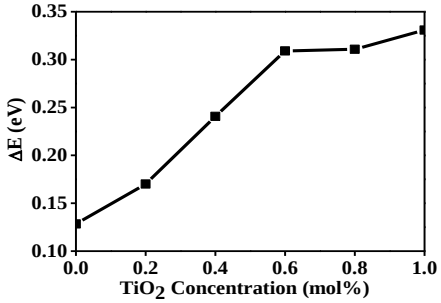

Figure 6 TiO_2 NPs concentration dependent Urbach energy

Figures 7 and 8 depict the TiO_2 NPs concentration dependent variation of refractive index and electronic polarizability, respectively. Introduction of TiO_2 increased the refractive index from 2.31 to 2.44. The increase of refractive index is interpreted in terms of the substitution of TeO^{4+} ions with Ti^{4+} ions. Addition of Ti^{4+} ions caused the reconstruction of tellurite network and increased the NBOs atoms that have higher polarizability than BOs [30]. Therefore, incorporation of TiO_2 NPs at higher concentration has enhanced the refractive index of the glass. An overall increase in polarizability with the addition of Ti^{4+} content is primarily ascribed to the creation of higher number of NBOs which have higher polarizability than BOs [8].

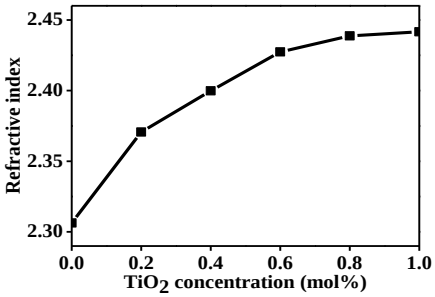

Figure 7 The refractive index against TiO_2 NPs concentration (mol %)

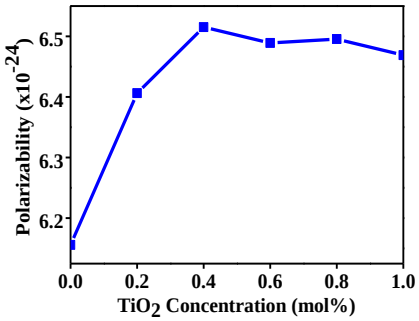

Figure 8 TiO_2 NPs concentration (mol %) dependent polarizability

4.0 CONCLUSION

TiO_2 NPs embedded erbium doped tellurite glasses acted as disordered plasmonic glass system are prepared and characterized. The impact of varying TiO_2 NPs concentration on physical and absorption properties are determined. The density and molar volume are found to vary in range of (5.18 - 5.07) g cm^{-3} and (26.31 - 26.80) m^3 mol^{-1}, respectively. SPR band of TiO_2 NPs is probed between 576 - 578 nm. The indirect and direct energy band gap are observed to decrease from (3.17 - 2.98) eV and (3.36 - 2.84) eV, respectively with the increase of TiO_2 NPs contents in the glass. The increase in Urbach energy in the range of (0.13 - 0.33) eV with the increase of TiO_2 NPs concentration is ascribed to the emergence of disorder via the creation of NBOs. Absorption features are observed to be modified with the incorporation of TiO_2 NPs. The improvement in absorption properties is attributed to the SPR mediated strong local field of TiO_2 NPs that appears in the close proximity of Er^{3+} ions. Our study may provide useful information towards the development of photonic devices based on Titania-Erbium-Tellurite plasmonic disordered glass system.

Acknowledgement

The authors gratefully acknowledge the financial support from UTM and Malaysian Ministry of Education through Vot. 05H36 (GUP) and 4F424 (FRGS).

References

[1] Seshadri, M., Chillcce, E. F., Marconi, J. D., Sigoli, F. a., *et al.* 2014. Optical Characterization, Infrared Emission and Visible Up-Conversion In Er^{3+} Doped Tellurite Glasses. *J. Non. Cryst. Solids*. 402: 141-148.

[2] Yusoff, N. M., Sahar, M. R., Ghoshal, S. K. 2015. Sm^{3+}:Ag NPs Assisted Modification in Absorption Features of Magnesium Tellurite Glass. *J. Mol. Struct.* 1079: 167-172.

[3] Stambouli, W., Elhouichet, H., Ferid, M. 2012. Study of Thermal, Structural and Optical Properties of Tellurite Glass With Different Tio_2 Composition. *J. Mol. Struct.* 1028: 39-43.

[4] Kenyon, A. J. 2002. Recent Developments in Rare-Earth Doped Materials for Optoelectronics. *Prog. Quantum Electron.* 26: 225-284.
[5] Dousti, M. R. 2013. Spectroscopic and Structural Properties of TeO_2 -ZnO-Na_2O-. *Chalcogenide.* 10: 411-420.
[6] Pal, U., Rodríguez, O. 2010. Ion Implantation for the Fabrication of Plasmonic Nanocomposites: A Brief Review. *cdn.intechopen.com*
[7] Abdulhalim, I., Zourob, M., Lakhtakia, A. 2013. Surface Plasmon Resonance for Biosensing: A Mini-Review. *Electromagnetics*. 28: 214-242.
[8] Stambouli, W., Elhouichet, H., Ferid, M. 2012. Study of Thermal, Structural And Optical Properties Of Tellurite Glass with Different TiO_2 Composition. *J. Mol. Struct.* 1028: 39-43.
[9] Farouk, M. 2014. Effect of TiO_2 On The Structural, Thermal and Optical Properties of BaO–Li_2O–Diborate Glasses. *J. Non. Cryst. Solids*. 402: 74-78.
[10] Peña-Rodríguez, O., Pal, U. 2011. Effects of Surface Oxidation on the Linear Optical Properties of Cu Nanoparticles. *J. Opt. Soc. Am. B*. 28: 2735.
[11] Shelby, J. E. 2005. *Introduction to Glass Science and Technology*. Royal Society of Chemistry.
[12] El-Diasty, F., Wahab, F. A. A., Abdel-Baki, M. 2006. Optical Band Gap Studies On Lithium Aluminum Silicate Glasses Doped With Cr^{3+} Ions. *J. Appl. Phys.* 100: 93511.
[13] Dimitrov, V., Komatsu, T. 1999. Electronic Polarizability, Optical Basicity and Non-Linear Optical Properties of Oxide Glasses. *J. Non. Cryst. Solids*. 249: 160-179.
[14] Eraiah, B., Bhat, S. G. 2007. Optical Properties Of Samarium Doped Zinc–Phosphate Glasses. *J. Phys. Chem. Solids*. 68: 581-585.
[15] El-Mallawany, R. 1999. Tellurite Glasses. *Mater. Chem. Phys.* 60: 103-131.
[16] Jlassi, I., Elhouichet, H., Ferid, M. 2011. Thermal and Optical Properties of Tellurite Glasses Doped Erbium. *J. Mater. Sci.* 46: 806-812.
[17] Mott, N. F., Davis, E. A. 2012. *Electronic Processes In Non-Crystalline Materials*. Oxford University Press.
[18] Urbach, F. 1953. The Long-Wavelength Edge of Photographic Sensitivity and of the Electronic Absorption of Solids. *Phys. Rev*. 92: 1324.
[19] Gayathri Pavani, P., Sadhana, K., Chandra Mouli, V. 2011. Optical, Physical and Structural Studies of Boro-Zinc Tellurite Glasses. *Phys. B Condens. Matter*. 406: 1242-1247.
[20] Dousti, M. R., Sahar, M. R., Ghoshal, S.K., Amjad, R.J., Arifin, R. 2012. Up-Conversion Enhancement In Er^{3+}-Ag Co-Doped Zinc Tellurite Glass: Effect of Heat Treatment. *J. Non. Cryst. Solids*. 358: 2939-2942.
[21] Ghoshal, S. K., Awang, A., Sahar, M. R., Arifin, R. 2015. Gold Nanoparticles Assisted Surface Enhanced Raman Scattering and Luminescence of Er^{3+} Doped Zinc–Sodium Tellurite Glass. *J. Lumin.* 159: 265-273.
[22] Sazali, E. S., Sahar, M. R., Ghoshal, S. K., Arifin, R., *et al.* 2014. Optical Properties of Gold Nanoparticle Embedded Er3+ Doped Lead–Tellurite Glasses. *J. Alloys Compd.* 607: 85-90.
[23] Awang, A., Ghoshal, S. K., Sahar, M. R., Arifin, R., Nawaz, F., 2014. Non-Spherical Gold Nanoparticles Mediated Surface Plasmon Resonance In Er^{3+} Doped Zinc-Sodium Tellurite Glasses: Role of Heat Treatment. *J. Lumin.* 149: 138-143.
[24] Jihong, Z., Haizheng, T., Yu, C., Xiujian, Z., Structure. 2007. Upconversion and Fluorescence Properties of Er3+-Doped TeO_2-TiO_2-La_2O_3 Tellurite Glass. *J. Rare Earths*. 25(Supple): 108-112.
[25] El-Mallawany, R., Abdalla, M.D., Ahmed, I.A. 2008. New tellurite glass: Optical properties. *Mater. Chem. Phys.* 109: 291-296.
[26] Rivera, V. A. G., Ledemi, Y., El-Amraoui, M., Messaddeq, Y., Marega, E. 2014. Control of the Radiative Properties Via Photon-Plasmon Interaction in Er^{3+}-Tm^{3+} -Codoped Tellurite Glasses in the Near Infrared Region. *Opt. Express.* 22: 21122-36.
[27] Malak, H. 2008. Plasmon-Enhanced Marking of Fragile Materials and Other Applications Thereof.
[28] Willets, K. a, Van Duyne, R. P. 2007. Localized Surface Plasmon Resonance Spectroscopy and Sensing. *Annu. Rev. Phys. Chem.* 58: 267-97.
[29] Kalele, S. A., Tiwari, N. R., Gosavi, S. W., Kulkarni, S. K. 2007. Plasmon-Assisted Photonics at the Nanoscale. *J. Nanophotonics*. 1: 12501-12520.
[30] Said Mahraz, Z. A., Sahar, M. R., Ghoshal, S. K., Reza Dousti, M. 2013. Concentration Dependent Luminescence Quenching Of Er3+-Doped Zinc Boro-Tellurite Glass. *J. Lumin.* 144: 139-145.
[31] Halimah, M. K., Daud, W. M., Sidek, H. A. A., Zaidan, A. W., Zainal, A. S. 2010. Optical Properties of Ternary Tellurite Glasses. *Mater. Sci. Pol.* 28: 173-180.